iVES OENO One vine & wine

DOI: https://doi.org/10.20870/oeno-one.2023.57.3.7251

OPEN ACCESS

ORIGINAL RESEARCH ARTICLE

Novel algorithms for high-resolution prediction of canopy evapotranspiration in grapevine

Matthew Jenkins[1], Autumn Mannsfeld[2], Shayla Nikzad[2], Jean-Jacques Lambert[3], Konrad Miller[2,3], Mark Burns[4], J. Mason Earles[3,5], and David E. Block[2,3]*

[1]Horticulture and Agronomy Graduate Group, University of California, One Shields Avenue, Davis, CA 95616, United States
[2]Department of Chemical Engineering, University of California, One Shields Avenue, Davis, CA 95616, United States
[3]Department of Viticulture and Enology, University of California, One Shields Avenue, Davis, CA 95616, United States
[4]Department of Chemical Engineering, University of Michigan, Ann Arbor, MI, United States
[5]Department of Biological and Agricultural Engineering, University of California, One Shields Avenue, Davis, CA 95616, United States

*correspondence: deblock@ucdavis.edu

Associate editor: Simone Castellarin

Received: 10 November 2022

Accepted: 31 August 2023

Published: 28 September 2023

ABSTRACT

Developing low-cost technology for custom water delivery to individual or small groups of plants is a critical next step to advance precision irrigation. Current systems for estimating evapotranspiration (ET), or plant water use, work on the scale of a full vineyard (e.g., 3–5 acres) or the scale of a single vine, but at a cost that prohibits monitoring past a small number of representative vines. To develop and evaluate low-cost ET sensors for individual grapevines, we used three head-pruned Zinfandel vines in pots and placed them on load cells to collect continuous weights indicative of actual ET. We mounted research-grade sensors for humidity, temperature, and wind speed on each vine and saved data at 2-minute intervals during three growing seasons. We developed three models based on first principles (Convective Mass Transfer or Mass Balance approaches) or simple correlations to predict actual single-plant ET from these data. We present here the results of a multi-year trial at the UC-Davis RMI vineyard to illustrate the performance of each of the models for ET estimation. Relative model performance was assessed by comparing model predictions to ground truth data provided by measurements from load cells–including assessments of estimated instantaneous ET rate, estimated cumulative water use over a one-hour window surrounding solar noon, and estimated cumulative water use over a full 24-hour period. The three algorithms developed consistently performed well, with single vine ET rate predictions showing a strong linear relationship with ground truth (range in r^2 over three seasons CMT r^2 = 0.61–0.86; MB r^2 = 0.07–0.91; EM r^2 = 0.57–0.92). The MB approach, which includes two measurements of relative humidity and temperature, was the most variable, likely due to the impact of sensor placement. In all seasons, we also examined the trend in the plant scaling factor found in each model, deemed A_s, which, based on model theory, is a function of vine size. Taken together, these results suggest that high-resolution irrigation (HRI) models are a promising new method for ET estimation at the single plant level.

KEYWORDS: evapotranspiration, modelling, high-resolution irrigation, mass balance, convective mass transfer, grapevine, irrigation management

INTRODUCTION

In California, recurrent droughts and water shortages have led to competition between agricultural, urban and conservation water needs (Diffenbaugh *et al.*, 2015). Even in the face of these challenges, there are still about 355,000 acres of grapes being cultivated throughout the state (CDFA and USDA, 2021). These vineyards typically use drip irrigation practices, which treat all plants in a management zone identically, even though it is clear that all plants do not require the same amount of water. Water demand heterogeneity can arise from cultivar differences, complex topography, canopy orientation, soil structure and composition, or rogueing practices for disease control, as examples. As a consequence of this variability, treating all plants in a management zone as identical will generally lead to some plants receiving excessive or inadequate water. Beyond the needs of the plant, water balance contributes to fruit quality and yield, layering additional complexity into its management. For example, in perennial woody crops like grapes and almonds, well-timed water stress can help control vegetative vigour and may increase fruit quality (Chaves *et al.*, 2007; Van Leeuwen and Seguin, 2006). Conversely, moderate to severe water stress caused by extreme deficit irrigation can damage cellular components for light harvesting, limiting photosynthesis. If this water stress is prolonged, delays in ripening, sudden vine collapse and reduced fruitfulness can negatively impact berry yield and quality (Dayer *et al.*, 2019). These constraints can create a problem, however, because the irrigation manager's goal is finding this narrow range of applied water by considering the plant's needs, but these needs usually vary in a complex way through space and time. When this variability is combined with complex deficit irrigation schemes, optimization of water use can be nearly impossible using existing technology.

1. Existing methods for measuring evapotranspiration

Current methods for measuring crop ET (ET_c) are powerful, and various approaches have already been commercialised. Some of the most widely used methods to measure ET are energy balance technologies, sap flow sensors, and the more traditional approach of reference ET (ET_o) and crop coefficients, but all of these methods come with significant limitations.

1.1. Energy balance technologies

Energy balance methods are based on the concept of conservation of energy, which states that the energy in some problem domain is constant. For the plant–soil–atmosphere system, then, energy balance theory states that net radiation must be in balance with the latent heat flux density, ground heat flux density, sensible heat flux density, and other less significant energy sinks. Ground heat flux density is the rate of heat storage in the soil and vegetation due to conduction and is either measured directly or computed using information from Normalized Difference Vegetation Index (NDVI) measurements. Sensible heat flux density is the energy lost to the air from the plant, soil and cover crops via convection and conduction. This term is sensitive to factors impacting the distribution of energy sources in the canopy, including wind speed and surface roughness, and is, therefore, affected by canopy size, structure, trellising, plant phenological stage and even ground surface heterogeneity (Rienth and Scholasch, 2019). Researchers have developed multiple methods to estimate sensible heat flux density, including eddy covariance, Bowen ratio method, and surface renewal (Li *et al.*, 2008; Paw *et al.*, 1995). The energy stored in the air layer, in the biomass, and chemical energy stored in the carbohydrate bonds of plant sugars are usually considered negligible compared to other terms (Anapalli *et al.*, 2018). The latent heat flux density is the heat lost from the system due to the evaporation of water and is calculated as a residual once all other parameters in the model are determined. Latent heat flux density divided by the latent heat of vaporisation of water will give ET.

While energy balance technologies for estimating ET_c are some of the most widely employed, they are also limited to coarse spatial resolutions, are expensive and can be sensitive to many different sources of error.

1.2. Sap flow sensors

Sap flow sensors are another promising technology with several advantages over energy balance methods. These sensors directly measure the movement of fluid inside the xylem from the roots to stems and to leaves, where water is transpired through stomata—a process called sap flow. Sap flow is essential for the maintenance of the hydraulic continuum from soil to plant to atmosphere; thus, monitoring this process can yield important information about the hydraulic function or dysfunction of the plant (Steppe *et al.*, 2015). Various methods for estimating sap flow rate have been developed, including thermal dissipation probes and the steam heat balance method (Granier, 1985; Lascano, 2000; Lascano *et al.*, 2016). Both are based on measuring the difference between a heated element and a non-heated reference element; as the sap flow rate increases, the temperature difference between the two elements decreases (Fernández and Testi, 2017). While the sap flow method will fundamentally achieve single-plant resolution, individual sensors are expensive and require skilled installation and routine maintenance labour. As a result, sensors are typically mounted on only 1 to 3 plants per management zone. Plants are chosen to represent the range of variability; a problematic assumption that can ignore many sources of heterogeneity.

1.3. Reference ET and crop coefficients

Another important method for estimating ET_c is by a proxy measurement along with correction factors known as crop coefficients, specific for the type of plant being grown nearby (Allan *et al.*, 1998; Behboudian and Singh, 2001). These proxy ET values, known as ET_o, are calculated at one of over 200 California Irrigation Management Information System (CIMIS) weather stations distributed throughout the state (Snyder and Sheradin, 2021); some other states have similar systems. Each station measures local weather parameters over a reference crop (well-watered grass), and these

parameters are fed into a Penman–Monteith model, which predicts hourly ET_o. Once ET_o is known, it can be used to calculate the true ET_c of crops grown nearby by multiplying by a scaling factor known as the crop coefficient (K_c). The crop coefficient is an experimentally derived value specific to the cultivar and is sometimes adjusted for other management factors (Bravdo, 1986). Compared to the other approaches for ET_c estimation, this method has the distinct advantage of being virtually free for California growers. However, this approach is limited by its reliance on the assumptions that regional ET_o values and crop coefficients are generalisable. As a result, this method can be quite effective at estimating regional ET_c, but it can lack local specificity, ignoring complex factors that influence slight differences in the vine-to-vine water demand, such as management practices, phenological stages, topography, soil characteristics and many others (Snyder and Sheradin, 2021). Additionally, these methods do not perform well under deficit irrigation when they cannot completely account for the response of plants to water stress (Hochberg *et al.*, 2017).

2. The High-Resolution Irrigation method

Our work addresses the complexity of modern irrigation management by outlining a system for delivering water differentially to each plant according to its needs—in other words, High-Resolution Irrigation (HRI). From the outset, we understood achieving HRI would require developing two fundamental components: (1) an engineered system for the targeted delivery of water to each plant and (2) an understanding of the plant's water needs that can inform irrigation decisions.

The second component, understanding a plant's water needs, requires knowing how much water to apply and when to apply it. The scope of this investigation is limited to exploring the question of how much water to apply, which is defined as evapotranspiration (ET) from a single plant.

Here, we introduce the development and theoretical basis of three novel HRI models for predicting ET rate. To illustrate the performance of each of the models, we present the results of a three-year trial at the UC Davis RMI vineyard. We assessed relative model performance, comparing instantaneous ET rate, cumulative water use over a one-hour window surrounding solar noon and cumulative water use over a full 24-hour period. Throughout the 2020, 2021 and 2022 growing seasons, we also examined the trend in the plant scaling factor found in each model, deemed A_s. Together, these observations strongly support the utility of the new HRI models for ET_c estimation.

MATERIALS AND METHODS

1. Collecting single vine data

We collected data from three head-trained *Vitis vinifera* L. cv. Zinfandel vines grafted on St. George rootstock (*V. rupestris*), planted in 1.1 m^3 plastic containers filled with Yolo County, CA sourced sandy loam. Zinfandel scion was grafted onto rootstock in Davis, CA, in 2009, and then vines were transplanted into containers in 2016. Yolo County sandy loam has been shown to have an available water holding capacity of about 10–15 % by volume (Schwankl and Prichard, 2009). Vines were located in the Robert Mondavi Institute (RMI) vineyard in Davis, California (Supplementary Figure 1). We irrigated vines using a dedicated programmable drip irrigation and fertigation system, composed of 8 equally spaced 2 L/H Woodpecker pressure compensating drippers (Netafim™, model 01WPC2) in a 1.5-meter circumference ring around the base of each vine. Irrigation events ranged in duration from 30 to 180 minutes and were programmed to occur before dawn every 24 to 72 hours during periods of normal irrigation, and no irrigation was done during dry-down periods. Vines received the same pest management and fertiliser regimen as other vines at RMI, per the direction of the vineyard manager. Data were collected from two vines during the 2020 and 2021 seasons and three vines in the 2022 season.

To predict the ET rate (units = kg • s^{-1}) and then calculate single plant ET (units = kg), we measured the wind speed, air temperature and relative humidity in vine canopies by mounting each vine with a suite of research-grade sensors. We measured wind speed (units m • s^{-1}) inside the vine canopy using a single needle anemometer (East 30 Sensors, Pullman, WA) that took instantaneous wind speed measurements every 10 seconds and recorded the average of the previous 12 instantaneous measurements for every 2-minute interval. We measured temperature (units °C) and relative humidity (units %) using HMP60L sensors (Campbell Scientific®, Logan, UT) mounted both inside and outside of each vine canopy and recorded instantaneous measurements at each 2-minute interval. We filtered all biometeorological data using a 3-hour moving average to remove noise without causing any significant over or under-approximation of daily maxima and minima.

To measure ground truth ET (units = kg), we placed each potted vine and attached sensor suite on a commercial load cell, model HFS 405 (2270 kg capacity, 0.01 kg resolution; CAS Corporation, Seoul, South Korea), which recorded instantaneous mass at each 2-minute interval. The load cell was calibrated each year in February using manufacturer guidelines. ET was then calculated by difference. From this point forward, ground truth ET will be referred to as load cell-measured ET. ET rate (units = kg • s^{-1}) is calculated by taking the derivative of mass with respect to time.

We automated all data collection using two CR1000 data loggers (Campbell Scientific®, Logan, UT), with 1 or 2 vines and associated sensors per logger, using custom CR1 programs. A single 30 W solar cell and 12 V lead acid battery powered the entire vine-sensor system.

2. Predicting ET rate for single grapevines

If the ET rate of water through the canopy of a plant could be measured, then calculating ET would be relatively straightforward. As current technology cannot accurately measure the ET rate directly at this scale, we have developed three novel models for predicting the ET rate using common biometeorological measurements.

These models estimate ET but do not include a term for soil evaporation as a first approximation because early experiments showed the effect of soil surface evaporation was small, averaging less than 5–10 % of daily water loss. Our methods use non-destructive, largely automated proximal sensing and a computation pipeline, feeding data from biometeorological sensors to the models. In this process, we measure wind speed, air temperature and relative humidity in or near the plant canopy. Using only these parameters, we have created three models, described in detail in the following sections, which can be used to calculate the estimated ET rate per area ($\dot{m}_e$, units kg • s^{-1} • m^{-2}) for single plants. Hereafter, we refer to the ET rate per area as mass flux.

2.1. Convective Mass Transfer mass flux model

The Convective Mass Transfer (CMT) model is one of two HRI models inspired by first principles. CMT relates transpiration to theory describing the convective mass transfer from a flat surface of water into moving air. This theory is based on applying the Reynolds analogy, which suggests a simple relationship between different transport phenomena (Cussler, 2009). In this case, we use an analogy to the well-described process of convective heat transfer from a flat solid plate into a fluid with laminar flow over its surface. Using this analogy, we can define transpiration as the convective mass transfer from a flat surface of liquid or a gas saturated with water vapour into a gas with laminar flow over its surface (Cussler, 2009). From this theory, the estimated mass transfer flux depends on the mass transfer coefficient (K_m) and the difference between the partial pressure of water in the air at the saturated surface (P_{sat}) and in the air in the greater atmosphere (P_∞) [Equation 1].

$$\dot{m}_e = K_m \cdot (P_{sat} - P_\infty)$$

In this case, the mass transfer coefficient (K_m) is a function of the mass diffusivity of air, the Reynolds number, the Schmidt number and a scalar term. The Reynolds number can be expressed as a function of the bulk velocity of air and kinematic viscosity, while the Schmidt number can be expressed as a function of kinematic viscosity and mass diffusivity. Note that in a pure gas, the diffusion coefficient and viscosity are proportional to $T^{3/2}$ and $T^{1/2}$, respectively (Bird *et al.*, 2006). When the pure gas condition is assumed to be true and all other constants are included in the scalar (k_{cmt}) term, the full CMT model can be reduced to [Equation 2]:

$$\dot{m}_e = v_\infty^{\frac{1}{2}} \cdot T^{\frac{11}{12}} \cdot k_{cmt} \cdot \Delta P$$

where v_∞ is the bulk velocity of air (m • s^{-1}) measured inside the canopy, T is canopy air temperature (K) and Δ P (g • m^{-2}) is the difference between partial pressure of water in air in the boundary layer and the greater atmosphere. The saturation pressure of water in the air is calculated using Antoine's Equation, which relates vapour pressure to air temperature and partial pressure is calculated by multiplying this value by relative humidity in the canopy. This model maintains three assumptions: first, all transpiring leaf surfaces are saturated with water vapour, perfectly flat and with a uniform temperature equal to the temperature of the air in the canopy. Second, stomata are assumed to remain in the open state to maintain constant boundary layer saturation and finally, it is assumed that a laminar flow of air exists at the leaf surface, which carries water vapour away from the boundary layer. Consistent with CMT theory, the area term (A_s) associated with this flux would be equal to the total saturated surface area of the transpiring leaves in the canopy. As k_{cmt} is a constant and not easily calculated a priori, here we will include this parameter with A_s to get a new modified area term, A_s', which will not affect the remainder of the analyses. Hence, in our calculations, Equation 2 is used without the k_{cmt} term.

2.2. Mass Balance mass flux model

The Mass Balance (MB) model is based on the concept of conservation of mass, which states that in any closed system, mass is constant and is neither created nor destroyed. In the case of a plant canopy, this means the mass flow rate of water out of the canopy ($\dot{m}_{out}$) is equal to the mass flow rate of water into the canopy ($\dot{m}_{in}$) plus the mass flow rate from the plant (i.e., evapotranspiration rate, $\dot{m}_p$). With rearrangement, this equation states the ET rate is equal to the difference between the mass flow rate out of the canopy and into the canopy, as seen in [Equation 3].

$$\dot{m}_p = \dot{m}_{out} - \dot{m}_{in} = (A_s \cdot v_{\infty,out} \cdot H_{out}) - (A_s \cdot v_{\infty,in} \cdot H_{in})$$

However, here, we assume that the cross-sectional area of the canopy is constant, as is the velocity of wind through the plant (verified experimentally). With these assumptions, the ET rate can be calculated as a product of the bulk velocity of air (v_∞, units m • s^{-1}) measured inside the canopy, the cross-sectional area of the canopy (A_s, units m^2) and the difference between the absolute humidity (H, units g • m^{-3}) outside and inside the canopy. Thus, by dividing both sides of Equation 3 by the area term, the full MB model for mass flux can be reduced to [Equation 4]:

$$\dot{m}_e = v_\infty \cdot \Delta H$$

where Δ H is the difference between H the air outside the canopy and the air inside the canopy. Absolute humidity, a function of air temperature, is computed using a formula derived from the Ideal Gas Law and an equation for Saturation Vapor Pressure (Snyder, 2005). As stated above, based on the mass balance concepts underlying this model, the area term (A_s) would equal the cross-sectional area of the vine canopy.

2.3. Empirical mass flux model

We selected the Empirical Model (EM) using only statistical methods from a set of more than 25 candidate models exploring mass flux as a function of various combinations of measured biometeorological parameters, as well as the interactions of these parameters. The goals of EM model development were generalisability and dimensional reduction. In addition to computational efficiency, dimensional reduction has the added benefit of reducing the number of sensors needed in the low-cost sensors being developed as part of this project.

We selected the full EM model [Equation 5] because, in addition to achieving reduced dimensionality, it also performed well in terms of ET predictions when compared to other candidate models.

$$\dot{m}_e = k_1 \cdot v_\infty + k_2 \cdot T + k_3 \cdot (v_\infty \cdot T)$$

The EM includes only bulk wind speed (v_∞, units m • s^{-1}) measured inside the canopy and air temperature (T, units °C) parameters, as well as the interaction of these parameters and unit fixing constants (k_1, k_2 and k_3). This approach assumes humidity measurements and related parameters (e.g., partial pressure) are not strong enough predictors of ET rate to be included in a model designed to explain variation in mass flux and inform irrigation decisions. Due to its empirical nature, the area term (A_s) in this model does not have a clear physical meaning.

3. Calculation of model area terms

To calculate ET_e (units = kg) from mass flux, the magnitude of the model-associated area term must first be measured or calculated; here, we calculated A_s experimentally. During any given time window, we achieved this calculation by dividing the load cell measured ET rate by the model-estimated mass flux. Throughout all seasons thus far, we used two to four continuous days of data to fit a new A_s term, then used this term to make projected predictions for the next 10–12 days. Based on data collected in 2020, we found that it is helpful to recalculate a new A_s term for each model every 10–14 days, at least until canopies are fully established.

4. ET_e from mass flux

Once mass flux has been calculated using one of the three novel models and A_s terms have been determined, it is possible to move on to ET calculation. Each HRI model generates an estimated instantaneous mass flux for every two-minute interval. This mass flux is integrated over time (t, units s) and multiplied by a plant scaling coefficient (A_s, units m^2), giving estimated ET_e [Equation 6]:

$$ET_e = A_s \cdot \int_0^t \dot{m}_e dt$$

ET rates are found by simply multiplying mass flux estimates by the A_s terms without integration. While early data suggests that all models perform well in terms of correlating estimated ET rate with measured ET rate, we have only started investigating methods for directly estimating the area term from physical measurements.

5. Programming and data analysis

For the following results, we used R v3.5.1 for all analysis and visualization (R Core Team, 2018). Model statistics, including r^2, p-value and RMSE, were generated using the 'stats' package, a part of R. For all computation, we used a 2021 Apple MacBook Pro with 16 gigabytes of random access memory.

RESULTS

From May 2020 through August 2022, we collected three seasons of data with our sensors and load cells. All biometeorological parameters are characterised by a strong diurnal pattern (Supplementary Figure 2). Ground truth ET data generated from load cell measurements were recorded at 2-minute intervals. When viewed over time, this data reveals periods of evapotranspiration as well as irrigation events (Supplementary Figure 3). The measured ET rate is computed from the load cell data by taking the derivative of mass with respect to time (Figure 1). It can be seen that the evapotranspiration is highest during times with peak temperature, which occurs around solar noon each day. While these data are reported only for a single vine, other vines exhibited very similar behaviour. Overall, we observed vines using about 30 litres of water per day, which falls within the range of observations from UC ANR in 2002, which measured 22.7 to 37.9 litres of water used per day for mature, vigorous grapevines in the Central Valley of California (Geisel *et al.*, 2002).

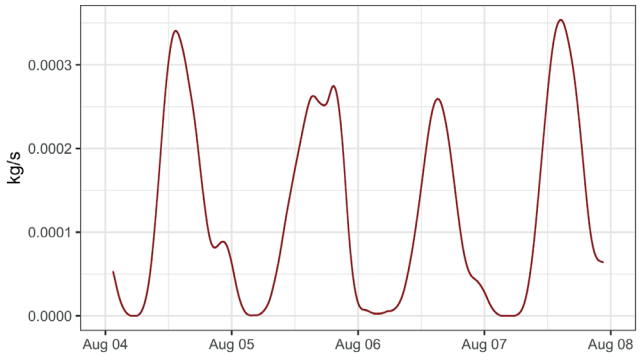

FIGURE 1. Load cell measured ET rate

[a]Measured ET rate is computed by taking the derivative of load cell mass with respect to time. Irrigation events were ignored using a filter. Data from August 2020

We used filtered biometeorological parameters to make ET rate predictions using our three models. In Figure 2, the load cell measured ET rate is plotted alongside the model-predicted ET rate over a 5-day period in June 2022. We found a strong linear relationship between model-predicted and load-cell-measured ET rates. The CMT predicted ET rate r^2 values were 0.89 for Vine 1, 0.85 for Vine 2 and 0.66 for Vine 3; MB predicted ET rate r^2 values were 0.78 for Vine 1, 0.22 for Vine 2 and 0.45 for Vine 3; and EM predicted ET rate r^2 values were 0.87 for Vine 1, 0.89 for Vine 2 and 0.74 for Vine 3 (Figure 2). We observed similar agreement over the course of the full 2020, 2021 and 2022 seasons (Table 1). At most times of the day, the CMT model tends to overpredict and the EM model tends to underpredict during the daytime and overpredict during night-time hours. The MB model was both under and overpredicted and was more prone to error. Importantly, we collected some of these data during extended periods of drought stress as well as during periods of typical irrigation.

TABLE 1. ET rate predictions over three years

Vine	Model	June 2020	July 2020	August 2020	June 2021	July 2021	August 2021	June 2022	July 2022	August 2022
1	CMT		Drydown			Drydown		Drydown		
		$r^2 = 0.73$	$r^2 = 0.84$	$r^2 = 0.82$	$r^2 = 0.78$	$r^2 = 0.75$	$r^2 = 0.68$	$r^2 = 0.86$	$r^2 = 0.78$	$r^2 = 0.73$
		RMSE = $1.04 \cdot 10^{-4}$	RMSE = $1.20 \cdot 10^{-4}$	RMSE = $1.03 \cdot 10^{-4}$	RMSE = $1.65 \cdot 10^{-4}$	RMSE = $2.38 \cdot 10^{-4}$	RMSE = $2.49 \cdot 10^{-4}$	RMSE = $1.20 \cdot 10^{-4}$	RMSE = $1.82 \cdot 10^{-4}$	RMSE = $1.73 \cdot 10^{-4}$
		p-value < $2 \cdot 10^{-16}$	p-value < $2 \cdot 10^{-16}$	p-value < $2 \cdot 10^{-16}$	p-value < $2 \cdot 10^{-16}$	pp-value < $2 \cdot 10^{-16}$	p-value < $2 \cdot 10^{-16}$	p-value < $2 \cdot 10^{-16}$	p-value < $2 \cdot 10^{-16}$	p-value < $2 \cdot 10^{-16}$
	MB		Drydown			Drydown		Drydown		
		$r^2 = 0.78$	$r^2 = 0.91$	$r^2 = 0.87$	$r^2 = 0.74$	$r^2 = 0.66$	$r^2 = 0.55$	$r^2 = 0.75$	$r^2 = 0.71$	$r^2 = 0.90$
		RMSE = $9.21 \cdot 10^{-5}$	RMSE = $9.20 \cdot 10^{-5}$	RMSE = $8.33 \cdot 10^{-5}$	RMSE = $1.70 \cdot 10^{-4}$	RMSE = $2.40 \cdot 10^{-4}$	RMSE = $2.81 \cdot 10^{-4}$	RMSE = $1.61 \cdot 10^{-4}$	RMSE = $1.47 \cdot 10^{-5}$	RMSE = $1.47 \cdot 10^{-5}$
		p-value < $2 \cdot 10^{-16}$	p-value < $2 \cdot 10^{-16}$	p-value < $2 \cdot 10^{-16}$	p-value < $2 \cdot 10^{-16}$	p-value < $2 \cdot 10^{-16}$	p-value < $2 \cdot 10^{-16}$	p-value < $2 \cdot 10^{-16}$	p-value < $2 \cdot 10^{-16}$	p-value < $2 \cdot 10^{-16}$
	EM		Drydown			Drydown		Drydown		
		$r^2 = 0.75$	$r^2 = 0.85$	$r^2 = 0.83$	$r^2 = 0.81$	$r^2 = 0.83$	$r^2 = 0.80$	$r^2 = 0.86$	$r^2 = 0.84$	$r^2 = 0.81$
		RMSE = $9.88 \cdot 10^{-5}$	RMSE = $1.19 \cdot 10^{-4}$	RMSE = $9.98 \cdot 10^{-5}$	RMSE = $1.52 \cdot 10^{-5}$	RMSE = $1.93 \cdot 10^{-4}$	RMSE = $1.94 \cdot 10^{-4}$	RMSE = $1.21 \cdot 10^{-4}$	RMSE = $1.56 \cdot 10^{-4}$	RMSE = $1.45 \cdot 10^{-4}$
		p-value < $2 \cdot 10^{-16}$	p-value < $2 \cdot 10^{-16}$	p-value < $2 \cdot 10^{-16}$	p-value < $2 \cdot 10^{-16}$	p-value < $2 \cdot 10^{-16}$	p-value < $2 \cdot 10^{-16}$	p-value < $2 \cdot 10^{-16}$	p-value < $2 \cdot 10^{-16}$	p-value < $2 \cdot 10^{-16}$
2	CMT		Drydown			Drydown		Drydown		
		$r^2 = 0.61$	$r^2 = 0.73$	$r^2 = 0.61$	$r^2 = 0.78$	$r^2 = 0.72$	$r^2 = 0.70$	$r^2 = 0.83$	$r^2 = 0.83$	$r^2 = 0.83$
		RMSE = $2.15 \cdot 10^{-4}$	RMSE = $1.01 \cdot 10^{-4}$	RMSE = $1.07 \cdot 10^{-4}$	RMSE = $1.33 \cdot 10^{-4}$	RMSE = $1.32 \cdot 10^{-4}$	RMSE = $1.47 \cdot 10^{-4}$	RMSE = $6.75 \cdot 10^{-5}$	RMSE = $7.01 \cdot 10^{-5}$	RMSE = $6.95 \cdot 10^{-5}$
		p-value < $2 \cdot 10^{-16}$	p-value < $2 \cdot 10^{-16}$	p-value < $2 \cdot 10^{-16}$	p-value < $2 \cdot 10^{-16}$	p-value < $2 \cdot 10^{-16}$	p-value < $2 \cdot 10^{-16}$	p-value < $2 \cdot 10^{-16}$	p-value < $2 \cdot 10^{-16}$	p-value < $2 \cdot 10^{-16}$
	MB		Drydown			Drydown		Drydown		
		$r^2 = 0.16$	$r^2 = 0.35$	$r^2 = 0.15$	$r^2 = 0.22$	$r^2 = 0.07$	$r^2 = 0.19$	$r^2 = 0.42$	$r^2 = 0.48$	$r^2 = 0.41$
		RMSE = $2.57 \cdot 10^{-4}$	RMSE = $1.56 \cdot 10^{-4}$	RMSE = $1.59 \cdot 10^{-4}$	RMSE = $2.35 \cdot 10^{-4}$	RMSE = $2.41 \cdot 10^{-4}$	RMSE = $2.41 \cdot 10^{-4}$	RMSE = $1.28 \cdot 10^{-4}$	RMSE = $1.24 \cdot 10^{-4}$	RMSE = $1.33 \cdot 10^{-4}$
		p-value < $2 \cdot 10^{-16}$	p-value < $2 \cdot 10^{-16}$	p-value < $2 \cdot 10^{-16}$	p-value < $2 \cdot 10^{-16}$	p-value < $2 \cdot 10^{-16}$	p-value < $2 \cdot 10^{-16}$	p-value < $2 \cdot 10^{-16}$	p-value < $2 \cdot 10^{-16}$	p-value < $2 \cdot 10^{-16}$
	EM		Drydown			Drydown		Drydown		
		$r^2 = 0.65$	$r^2 = 0.67$	$r^2 = 0.57$	$r^2 = 0.86$	$r^2 = 0.88$	$r^2 = 0.89$	$r^2 = 0.87$	$r^2 = 0.92$	$r^2 = 0.89$
		RMSE = $2.02 \cdot 10^{-4}$	RMSE = $1.04 \cdot 10^{-4}$	RMSE = $1.12 \cdot 10^{-4}$	RMSE = $9.85 \cdot 10^{-5}$	RMSE = $8.38 \cdot 10^{-5}$	RMSE = $8.65 \cdot 10^{-5}$	RMSE = $5.93 \cdot 10^{-5}$	RMSE = $4.87 \cdot 10^{-5}$	RMSE = $5.79 \cdot 10^{-5}$
		p-value < $2 \cdot 10^{-16}$	p-value < $2 \cdot 10^{-16}$	p-value < $2 \cdot 10^{-16}$	p-value < $2 \cdot 10^{-16}$	p-value < $2 \cdot 10^{-16}$	p-value < $2 \cdot 10^{-16}$	p-value < $2 \cdot 10^{-16}$	p-value < $2 \cdot 10^{-16}$	p-value < $2 \cdot 10^{-16}$

*Data are shown for Vine 1 (V1) and Vine 2 (V2) for the months of June, July and August in 2020, 2021 and 2022 growing seasons. Each cell gives the r^2, RMSE, and p-value for the relationship between model predicted ET rate and load cell measured ET rate. The cells marked "Drydown" included a 10-day drydown. Two vines were used because only two vines of data were available for all three seasons.

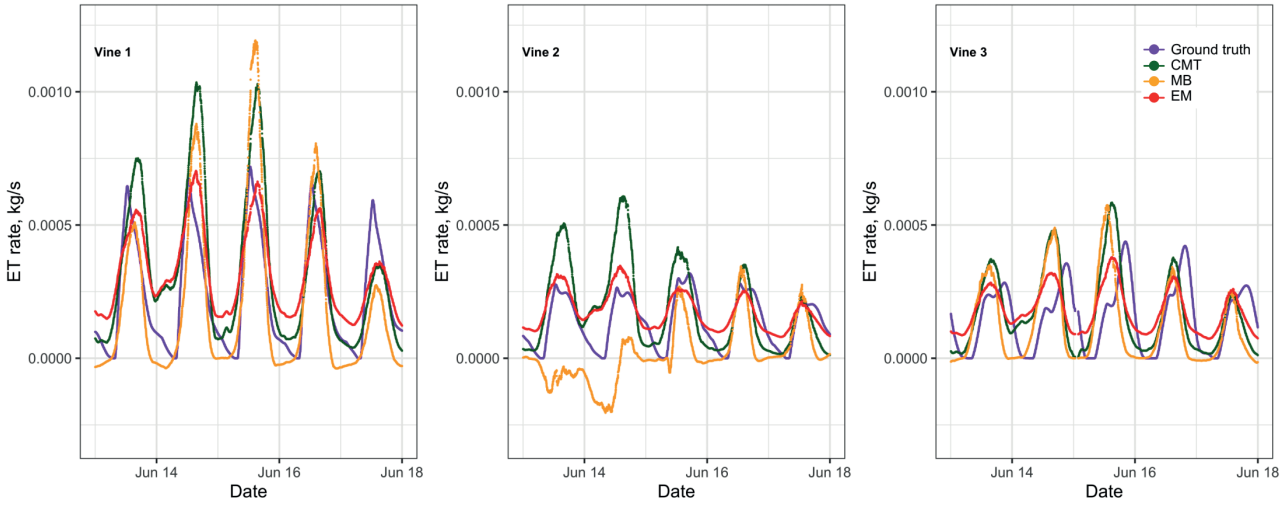

FIGURE 2. Predicted and measured ET rates over time

[a]Each plot shows the ET rate of water as determined by the load cell and by one the HRI models for a 5-day period in June 2022. In all figures, the purple line represents the load cell measured ET rate. The p-value for all linear regressions was less than $2 \cdot 10^{-16}$. The CMT r^2 values ranged from 0.66 to 0.89, the MB r^2 values ranged from 0.22 to 0.78, and the EM r^2 values ranged from 0.74 to 0.89. An expanded version of Figure 2 is available in the Supplementary Figures section as Supplementary Figure 4, and includes r^2, p-value, and linear regression equations, for each vine and model.

Including stressful periods, noted in Table 1, provides additional evidence that the models generate estimates of crop ET_c and not another concept like reference ET_o, which is more related to evaporative demand. In this experiment, each dry-down event represents 10 consecutive days without receiving any applied irrigation. Note the relatively poor performance of Vine 2 in the MB model in all growing seasons, exhibited in Figure 2 and Table 1. This can be attributed to errors when calculating absolute humidity differences from temperature and individual relative humidity, especially when these differences are small. Sometimes, when absolute humidity inside and outside the canopy is very close, a negative ET rate can be calculated, which is unlikely for grapevine and is probably a result of a lack of sensitivity in the methods used to sense and calculate absolute humidity. Absolute humidity error could also be the result of sensor placement. We noted the outside canopy relative humidity sensors for Vine 2 were placed upwind of prevailing winds relative to Vine 2, while the outside canopy humidity sensors for Vine 1 and 3 were placed downwind relative to their respective vines, thus indicating the importance of proper sensor placement for the successful use of the MB approach. Both the CMT and EM models give generally good predictions of the ET rate. Neither of these approaches uses the external relative humidity sensors on the experimental vines, which means none of the effects seen on Vine 2 are present in these calculations.

Given their physical bases, we hypothesised that the trend in the CMT and MB associated A_s terms over each season could have a consistent relationship to the seasonal trend in other plant physical parameters, such as Leaf Area Index (LAI) or cross-sectional area of the canopy (Orlando *et al.*, 2016; Figure 3). In 2020 and 2022, the CMT model A_s values displayed an overall trend that somewhat or very much resembles annual cycles in canopy physical parameters like LAI, with an increase until approximate veraison with subsequent levelling out, but this trend was reversed in 2021. While in 2022, the MB model A_s trend was somewhat like the expected trend, the trends observed in 2020 and 2021 were not what we would expect for plant growth during a growing season. In several instances during 2020 and 2021, the MB model A_s values were below zero, indicating erroneous predictions likely due to sensitivity issues with sensing and calculating absolute humidity. After these observations, we now believe that the A_s term relationship to physical measurements, such as LAI, is more nuanced and is likely mediated by other factors, such as physiological changes caused by the senescence of older leaves, fruit set, or other seasonal processes.

With the calculation of A_s terms, we can now directly compare the load cell measured and model predicted ET. Load cell measured ET, ET_c, is calculated by integrating load cell measured ET rate over time. For all vines, we computed the model predicted ET_e and load cell measured ET_c over a 1-hour window from 13:00–14:00 PST, daily using 56 days for Vine 1, 42 days for Vine 2 and 23 days for Vine 3, distributed approximately evenly from May to August 2022 (Figure 4). The days used to calculate model predicted ET_e and load cell measured ET_c were chosen based on the availability of a continuous set of data for a full 24-hour period. The main challenge to finding a full 24 hours of measurements every 2 minutes was frequent gaps in wind speed data, a result of the unprotected needle design of the anemometers. If the anemometer needle comes into contact with anything, such as a leaf, insect or debris, during the measurement window, it will record a zero, negative or unreasonably large value. These erroneous recordings are considered to be gaps or missing data. To understand how the models performed relative to one another over short periods of time during the day, we performed multiple linear regression analyses on all 1-hour vine and model data.

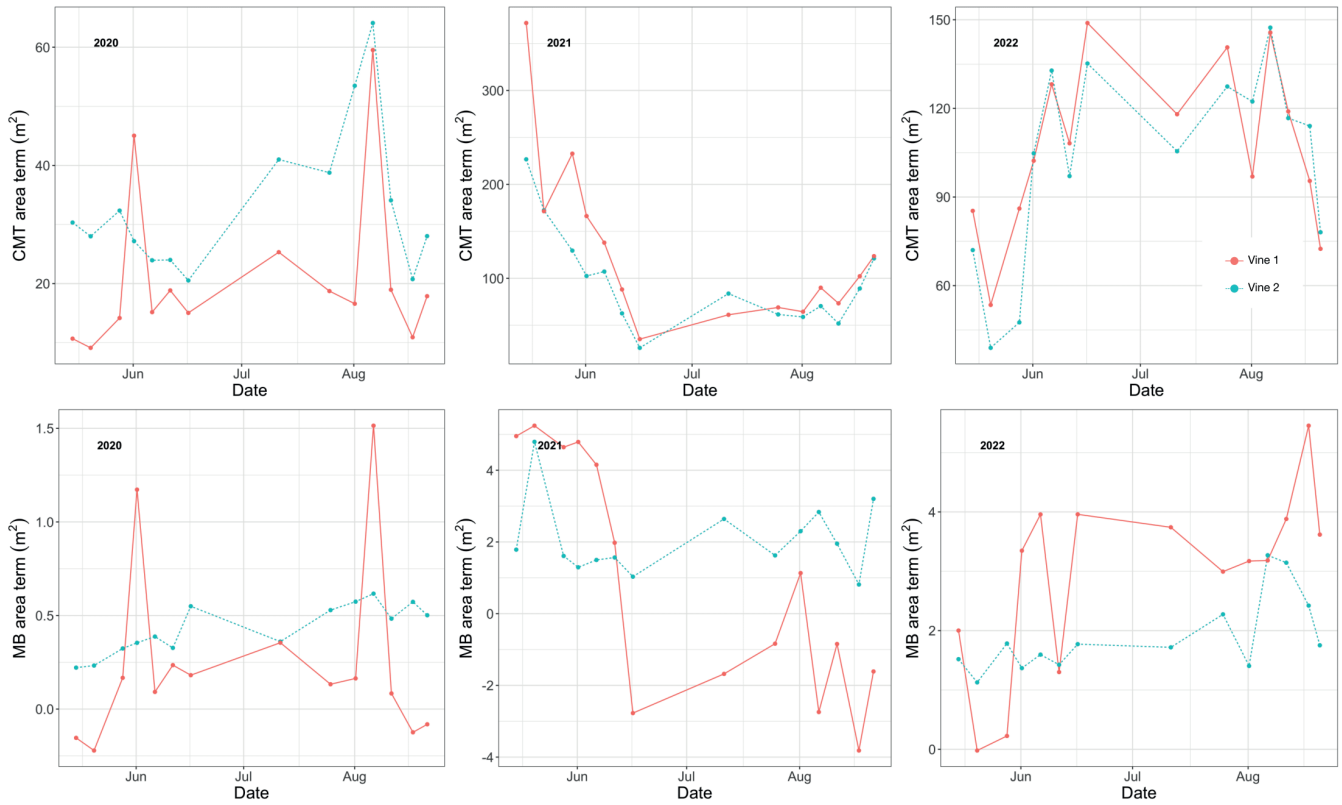

FIGURE 3. CMT and MB model area terms over three years

▫Example of trend in experimentally determined area term (As) values for CMT (top row) and MB (bottom row) models over the 2020 (left column), 2021 (middle column), and 2022 (right column) growing seasons. Legend in top, right panel

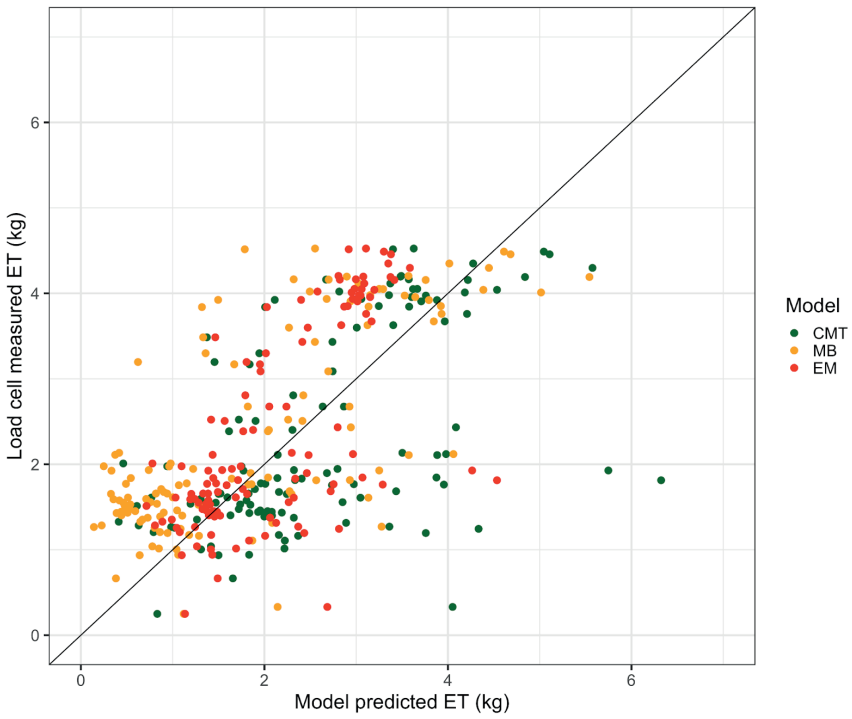

FIGURE 4. Predicted vs. measured ET over 1 hour window

▫Plot comparing the predicted ET_e from all of the HRI models, and ground truth ET_c from the load cells during a 1 hour window from 13:00–14:00 each day (units = kg). Data are from Vines 1–3 using dates May–August in the 2022 season. Data were fit with a multiple linear regression model, and a 1:1 reference line is shown in black. The multiple r-squared is 0.6292, and all model associated p-values are significant at the 0.001 level of significance.

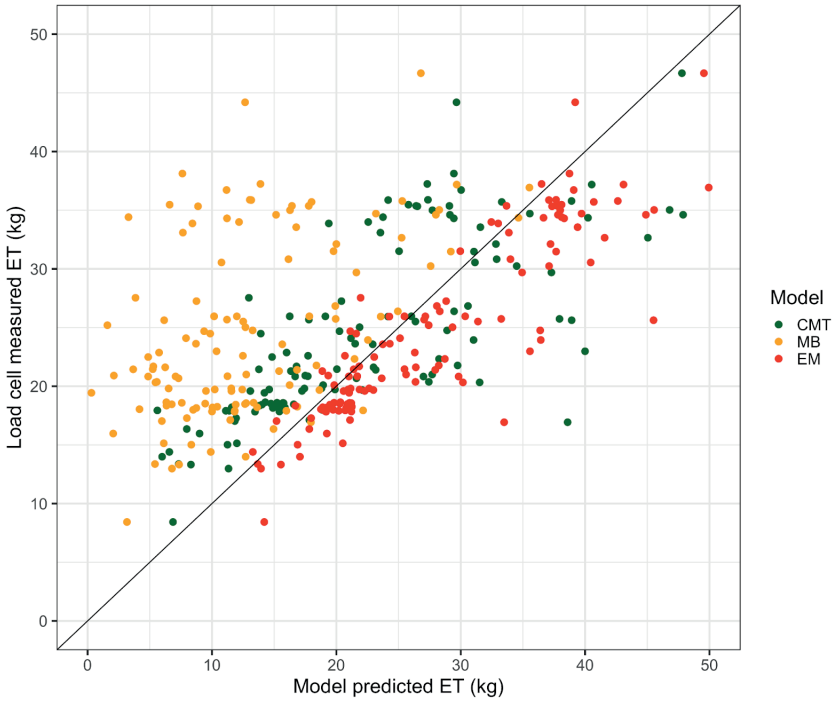

FIGURE 5. Predicted vs. measured ET over 24 hour window

[a]Plot comparing the predicted ET_e from all of the HRI models, and ground truth ET_c from the load cells during a 24 hour window each day (units = kg). Data are from Vines 1–3 using dates May–August in the 2022 season. Data were fit with a multiple linear regression model, and a 1:1 reference line is shown in black. The multiple r-squared is 0.8232, and the CMT and EM model associated p-values are significant at the 0.001 level of significance. The MB model p-value is 0.17.

The multiple r-squared is 0.6292, suggesting a good overall fit, and all model p-values are significant at the 0.001 level, indicating a significant relationship between all model predictions and ground truth.

We also computed the model-predicted ET_e and load cell measured ET_c over a 24-hour window, daily for the same 23, 42 or 56 days distributed approximately evenly from May to August 2022 (Figure 5). With the inclusion of night in this multiple linear regression analysis, when little to no ET is occurring, and all models predict more accurately than during the day, the linear relationships between model predicted and ground truth ET now explain up to 82 % of the variation in crop ET_c over a wide range of phenological stages and environmental conditions. The increase in explained variation could also be due to small shifts in prediction compared to ground truth. These shifts have a relatively large effect on the accuracy of predictions during some times of day, but over longer integration periods, this effect is significantly reduced. Overall, only the CMT and EM model p-values are significant at the 0.001 level. MB model predictions are associated with a p-value of 0.17, suggesting a non-significant relationship between MB-predicted ET and ground truth ET over full 24-hour periods.

We suggest, based on these results, that crop ET can be modelled effectively using HRI techniques and biometeorological data measured in vine canopies, though accurate calculation of A_s values may be critical to improving these predictions and enhancing generalisability.

DISCUSSION

Given the generally consistent results over multiple seasons, we believe the three novel HRI models for predicting the ET rate of a single vine are a promising new method. With this fine-scale understanding of the water use of individual plants, irrigation managers could, for the first time, adjust water application rates to ensure plants are receiving what they need and nothing more. This vital step towards improved efficiency of applied irrigation, which accounts for the vine-to-vine water use variability that results from the heterogeneity of vineyards, will support further development of important technology capable of addressing the growing problem of water scarcity while maintaining or improving grape quality.

The data presented here is strong evidence that the ET rate can be well described using only simple biometeorological measurements and either first principles or empirical models. Based on the performance criteria of r^2 and RMSE, the EM model consistently explained more variation in ET rate than other models. However, while the EM gave the best results for these vines, we believe that the CMT model or MB models, which are based on first principles, will prove to be more generalizable, especially to variable canopy architectures and seasonal changes.

Other technologies designed to estimate ET also face challenges, but comparing other models to the HRI model is not straightforward because most other models make predictions at coarser time scales.

Generally, data from other ET estimation methods, especially crop coefficient methods, is presented on the scale of months or seasons, such as in Li *et al.* (2008), not days or hours. However, in Gómez-Candón *et al.* (2021), researchers captured multispectral images of Durum wheat fields using UAVs and then calculated actual ET using a Two-Source Energy Balance, an application of energy balance which separates energy fluxes, and, therefore, ET, from plant and soil into two components (Norman *et al.,* 1995; Kustas and Anderson, 2009). Using this method, the remotely sensed estimates of ET calculated with the TSEB model only explained 50 % of the variation in daily ground truth ET measurements. While these researchers exemplified how challenging applying ET sensing methods can be in the field, some studies have also reported better performance of the energy balance approach. Anapalli *et al.* (2018) demonstrated energy balance ET predictions can explain as much as 82 % of the variation in lysimeter ET; however, this study was focused on corn and the ET measurements were less frequent, at once per day. Still, comparing these correlations to those observed in Table 1, it is reasonable to conclude that the HRI models offer a viable alternative to existing methods for estimating ET.

While the observed correlations with ET rate persist over multiple vines and multiple seasons, accurate prediction of ET_e will depend on the accurate calculation of the A_s term, which may vary with plant and over time. The A_s terms for two of the models, CMT and MB, have an actual physical meaning, albeit with the CMT model term incorporating k_{cmt}, but measuring those parameters directly may not be straightforward and will require further exploration. Again, for a single vineyard, we may not need this term to make good predictions of ET, but to make these predictions generalisable, it will be essential, especially if vines are of different sizes because of replanting or heterogeneities in soil or topography. Calculation of A_s terms directly from physical data, such as ground-based imagery of the vines collected throughout the season during normal tractor passes, would be possible. Downstream image analysis could be automated using a deep learning approach, similar to the approach used in Olenskyj *et al.* (2022), to extract canopy cross-sectional areas, total leaf area, or other physical parameters of the vine that are well correlated with the model A_s terms.

Because generalisability is likely a prerequisite for the viability of this technology, it is critical that we unravel the physical meaning of this term and how to measure it directly. Studying how the experimentally derived A_s terms change over the growing season provides early insights into how we might overcome this problem. As was previously mentioned, we believe the trend in the area term could have some consistent relationship to the trend of other plant physical parameters over the growing season, such as leaf area or leaf area index, which tends to increase until harvest (typically early September in California) when it begins decreasing until leaves are shed shortly thereafter (Netzer *et al.*, 2009). Given these observations and the physical basis of two of the HRI models, we hypothesised that the A_s term will be proportional to other physical measurements such as LAI or canopy cross-section. However, the experimentally derived area terms from the 2021 season did not resemble the expected pattern. Due to the way humidity and temperature sensors were mounted in the centre of the canopy and not in a different or more dynamic position, we believe the calculations of true A_s were masked by other intracanopy effects, such as physiological changes in transpiration rate caused by senescence of older leaves, fruit set, or other seasonal processes. In future studies, we aim to explore ways to mitigate the effect of these other variables.

Other challenges include issues with the relative placement of humidity sensors and vines, which can severely impact the accuracy of MB-predicted mass flux. In future seasons, we will investigate more accurate methods for calculating absolute humidity, including methods that are not sensitive to the relative positioning of vines and sensors or, alternatively, finding the optimal location of sensors for a given vine geometry. This issue is exemplified in Figure 2 and Table 1, which both show the MB predicted ET rate for Vine 2 as underperforming relative to other vines. Moreover, note that in Figure 3, the A_s term for the MB predictions dips below 0 several times in 2020 and 2021, indicating a negative ET rate was erroneously calculated. This sensitivity to sensor and vine location reveals a fundamental weakness of the MB model, as it requires twice as many sensors as the other models and ideal sensor placement, and, therefore, increases the likelihood of incorrect measurements.

In addition to these issues, implementation in a commercial vineyard presents other challenges. For example, it is possible that canopies with less radial symmetry, such as many common trellis systems in California, could be more difficult to measure. It is also possible that certain trellis systems, cultivars, regions, topographical features, or other factors we have yet to consider could limit the performance of the models. In addition, sensors used by the models will need to be inexpensive, especially if every vine or a high density of vines is to be monitored, and robust in an agricultural environment—both topics of further research.

CONCLUSION

Even with the remaining challenges of increasing generalizability, the algorithms' prediction of the ET rate of water from single vines is very promising as an inexpensive and high-resolution means of controlling irrigation. Applied correctly, the algorithms presented here provide an option to growers looking for greater efficiency of irrigation and improved crop quality. The HRI algorithms provide a theoretical and practical basis for growers to balance irrigation with the varied water demands of vines growing in heterogeneous environments, all using a non-invasive and automated process.

ACKNOWLEDGEMENTS

The authors thank Leticia Chacon Rodriguez for viticultural guidance and access to vineyard facilities, Guillermo Federico Garcia Zamora and Gonzalo Ruiz Gonzalez for assistance with vine care and equipment installation at the

RMI Vineyard, and Kathryn Prendergast of the Graduate Writing Fellows at the University of California Davis for assistance with editing. This work was made possible through financial support from Till Guldimann and the Ernest Gallo Endowed Chair in Viticulture and Enology.

AUTHOR CONTRIBUTIONS

M.R.J., J.J.L., S.N. and D.E.B. designed and implemented the experimental field setup. K.M. and M.R.J. conceptualised the CMT model. D.E.B., S.N. and M.R.J. conceptualised the MB model. M.R.J. conceptualised the EM model. M.R.J. and A.M. wrote all the code for data capture, analysis and visualisation. M.R.J. and D.E.B. wrote the paper with revisions from all authors. D.E.B., M.B., J.J.L. and J.M.E. provided funding and access to materials.

DATA AVAILABILITY

Some of the data used for this publication, including examples from all sensors and the load cell, is available as a CSV file on Zenodo at https://doi.org/10.5281/zenodo.7983157.

REFERENCES

Allan, R., Pereira, L., & Smith, M. (1998). *Crop evapotranspiration-Guidelines for computing crop water requirements-FAO Irrigation and drainage paper 56* (Vol. 56). http://www.climasouth.eu/sites/default/files/FAO%2056.pdf

Anapalli, S. S., Green, T. R., Reddy, K. N., Gowda, P. H., Sui, R., Fisher, D. K., Moorhead, J. E., & Marek, G. W. (2018). Application of an energy balance method for estimating evapotranspiration in cropping systems. *Agricultural Water Management, 204*, 107–117. https://doi.org/10.1016/j.agwat.2018.04.005

Behboudian, M. H., & Singh, Z. (2001). *Water Relations and Irrigation Scheduling in Grapevine. In Horticultural Reviews* (pp. 189–225). John Wiley & Sons, Ltd. https://doi.org/10.1002/9780470650813.ch5

Bird, R. B., Stewart, W. E., & Lightfoot, E. N. (2006). *Transport Phenomena*. John Wiley & Sons. https://doi.org/10.1002/aic.690070245

Bravdo, B. (1986). Water management and effect on fruit quality in grapevines. Proceedings of the 6th Australian wine industry technical conference, 1(9), 150-158. https://awitc.com.au/program/proceedings/sixth-australian-wine-industry-technical-conference/

CDFA, & USDA (2021). California Department of Food and Agriculture in cooperation with USDA National Agricultural Statistics Service. *Grape Acreage Report 2021. 34*(1). 2-4. https://www.nass.usda.gov/Statistics_by_State/California/Publications/Specialty_and_Other_Releases/Grapes/Acreage/2022/2021gabtb.pdf

Chaves, M.M., Santos, T. P., Souza, C. R., Ortuño, M. F., Rodrigues, M. L., Lopes, C. M., Maroco, J. P., & Pereira, J. S. (2007). Deficit irrigation in grapevine improves water use efficiency while controlling vigour and production quality. *Annals of Applied Biology, 150*(2). 237-252. https://doi.org/10.1111/j.1744-7348.2006.00123.x

Cussler, E. L. (2009). *Diffusion: Mass Transfer in Fluid Systems*. Cambridge University Press. https://doi.org/10.1017/CBO9780511805134

Dayer, S., Reingwirtz, I., McElrone, A.J., & Gambetta, G.A. (2019). Response and Recovery of Grapevine to Water Deficit: From Genes to Physiology. In: Cantu, D., Walker, M. (eds) *The Grape Genome. Compendium of Plant Genome*s. Springer, Cham. https://doi.org/10.1007/978-3-030-18601-2_11

Diffenbaugh, N. S., Swain, D. L., & Touma, D. (2015). Anthropogenic warming has increased drought risk in California. *Proceedings of the National Academy of Sciences, 112*(13), 3931–3936. https://doi.org/10.1073/pnas.1422385112

Fernández, E., & Testi, L. (2017). *Methods to Estimate Sap Flow*. ISHS Working Group on Sap Flow, 9(1). Article 09. https://www.ishs.org/sites/default/files/documents/methods_0.pdf

Hochberg, U., Herrera, J., Degu, A., Castellarin, S. D., Peterlunger, E., Alberti, G., & Lazarovitch, N. (2017). Evaporative demand determines the relative transpirational sensitivity of deficit-irrigated grapevines. *Irrigation Science, 35*. https://doi.org/10.1007/s00271-016-0518-4

Geisel, P., Farnham, D., & Vossen, P. (2002). *California Master Gardener Handbook (3338th ed.)*. University of California, Division of Agriculture and Natural Resources.

Gómez-Candón, D., Bellvert, J., & Royo, C. (2021). Performance of the Two-Source Energy Balance (TSEB) Model as a Tool for Monitoring the Response of Durum Wheat to Drought by High-Throughput Field Phenotyping. *Frontiers in Plant Science, 12*. https://www.frontiersin.org/articles/10.3389/fpls.2021.658357

Granier, A. (1985). Une nouvelle méthode pour la mesure du flux de sève brute dans le tronc des arbres. *Annales des Sciences Forestières, 42*(2), 193–200. https://doi.org/10.1051/forest:19850204

Kustas, W., & Anderson, M. (2009). Advances in thermal infrared remote sensing for land surface modeling. *Agricultural and Forest Meteorology, 149*(12), 2071–2081. https://doi.org/10.1016/j.agrformet.2009.05.016

Paw, U. K.T., Qiu, J., Su, H.-B., Watanabe, T., & Brunet, Y. (1995). Surface renewal analysis: A new method to obtain scalar fluxes. *Agricultural and Forest Meteorology, 74*(1), 119–137. https://doi.org/10.1016/0168-1923(94)02182-J

Lascano, R. J. (2000). A General System to Measure and Calculate Daily Crop Water Use. *Agronomy Journal, 92*(5), 821–832. https://doi.org/10.2134/agronj2000.925821x

Lascano, R. J., Goebel, T. S., Booker, J., Baker, J. T., & Gitz III, D. C. (2016). The Stem Heat Balance Method to Measure Transpiration: Evaluation of a New Sensor. *Agricultural Sciences, 07*(09), Article 09. https://doi.org/10.4236/as.2016.79057

Li, S., Kang, S., Li, F., & Zhang, L. (2008). *Evapotranspiration and crop coefficient of spring maize with plastic mulch using eddy covariance in northwest China*. https://doi.org/10.1016/j.agwat.2008.04.014

Netzer, Y., Yao, C., Shenker, M., Bravdo, B.-A., & Schwartz, A. (2009). Water use and the development of seasonal crop coefficients for Superior Seedless grapevines trained to an open-gable trellis system. *Irrig. Sci., 27*, 109–120. https://doi.org/10.1007/s00271-008-0124-1

Norman, J. M., Kustas, W. P., & Humes, K. S. (1995). Source approach for estimating soil and vegetation energy fluxes in observations of directional radiometric surface temperature. *Agricultural and Forest Meteorology, 77*(3), 263–293. https://doi.org/10.1016/0168-1923(95)02265-Y

Olenskyj, A., Sams, B., Fei, Z., Singh, V., Raja, P., Bornhorst, G., & Earles, J.M. (2022). *End-to-end deep learning for directly estimating grape yield from ground-based imagery*. arXiv. https://arxiv.org/abs/2208.02394

Orlando, F., Movedi, E., Coduto, D., Parisi, S., Brancadoro, L., Pagani, V., Guarneri, T., & Confalonieri, R. (2016). Estimating Leaf Area Index (LAI) in Vineyards Using the PocketLAI Smart-App. *Sensors (Basel, Switzerland), 16*(12). https://doi.org/10.3390/s16122004

R Core Team (2018). R: A language and environment for statistical computing. *R Foundation for Statistical Computing*. https://www.r-project.org/

Rienth, M., & Scholasch, T. (2019). State-of-the-art of tools and methods to assess vine water status. *OENO One, 53*(4), Article 4. https://doi.org/10.20870/oeno-one.2019.53.4.2403

Schwankl, L. J., & Prichard, T. (2009). *Understanding Water Holding Characteristics*. University of California Drought Management Web Site. http://UCManageDrought.ucdavis.edu

Snyder, R. L. (2005). Humidity Conversion. *UC Davis Biometeorology Group, 2*(1), 2-5. https://www.slideshare.net/AliAli127/hum-con

Snyder, R.L., & Sheradin, H.L. (2021). Water Balance Irrigation Scheduling Using CIMIS ETo: Department of Land, Air and Water Resources—UC Davis. (n.d.). Retrieved May 17, 2021, from https://lawr.ucdavis.edu/cooperative-extension/irrigation/drought-tips/water-balance-irrigation-scheduling-using-cimis-eto

Steppe, K., Vandegehuchte, M., Tognetti, R., & Mencuccini, M. (2015). Sap flow as a key trait in the understanding of plant hydraulic functioning. *Tree Physiology, 35*(4), 341–345. https://doi.org/10.1093/treephys/tpv033

Van Leeuwen, C. & Seguin, G. (2006). The concept of terroir in viticulture. *Journal of Wine Research, 17*(1). 1-10. https://doi.org/10.1080/09571260600633135